

Effect of solution pH, ionic strength, and temperature on adsorption behavior of reactive dyes on activated carbon

Yahya S. Al-Degs^a, Musa I. El-Barghouthi^a, Amjad H. El-Sheikh^a, Gavin M. Walker^{b,*}

^a Chemistry Department, The Hashemite University, P.O. Box 150459, Zarqa, Jordan

^b School of Chemistry and Chemical Engineering, Queen's University Belfast, David Keir Building, Stranmillis Road, Belfast, Northern Ireland BT9 5AG, UK

Received 7 September 2006; received in revised form 28 February 2007; accepted 2 March 2007

Available online 12 March 2007

Abstract

The adsorption behavior of C.I. Reactive Blue 2, C.I. Reactive Red 4, and C.I. Reactive Yellow 2 from aqueous solution onto activated carbon was investigated under various experimental conditions. The adsorption capacity of activated carbon for reactive dyes was found to be relatively high. At pH 7.0 and 298 K, the maximum adsorption capacity for C.I. Reactive Blue 2, C.I. Reactive Yellow 2 and C.I. Reactive Red 4 dyes was found to be 0.27, 0.24, and 0.11 mmol/g, respectively. The shape of the adsorption isotherms indicated an L2-type isotherm according to the Giles and Smith classification. The experimental adsorption data showed good correlation with the Langmuir and Ferundlich isotherm models. Further analysis indicated that the formation of a complete monolayer was not achieved, with the fraction of surface coverage found to be 0.45, 0.42, and 0.22 for C.I. Reactive Blue 2, C.I. Reactive Yellow 2 and C.I. Reactive Red 4 dyes, respectively. Experimental data indicated that the adsorption capacity of activated carbon for the dyes was higher in acidic rather than in basic solutions, and further indicated that the removal of dye increased with increase in the ionic strength of solution, this was attributed to aggregation of reactive dyes in solution. Thermodynamic studies indicated that the adsorption of reactive dyes onto activated carbon was an endothermic process. The adsorption enthalpy (ΔH_{ads}) for C.I. Reactive Blue 2 and C.I. Reactive Yellow 2 dyes were calculated at 42.2 and 36.2 kJ/mol, respectively. The negative values of free energy (ΔG_{ads}) determined for these systems indicated that adsorption of reactive dyes was spontaneous at the temperatures under investigation (298–328 K).

© 2007 Elsevier Ltd. All rights reserved.

Keywords: Reactive dyes; Activated carbon; Adsorption; pH_{pzc}

1. Introduction

There are more than 1,00,000 types of dyes commercially available, with over 7×10^5 tonnes of dyestuff produced annually, which can be classified according to their structure as anionic and cationic [1]. In aqueous solution, anionic dyes carry a net negative charge due to the presence of sulphonate (SO_3^-) groups, while cationic dyes carry a net positive charge due to the presence of protonated amine or sulfur containing groups [2]. Due to their strong interaction with many surfaces of synthetic and natural fabrics, reactive dyes are used for dyeing

wool, cotton, nylon, silk, and modified acrylics [3]. Discharging dyes into the hydrosphere can cause environmental damage as the dyes give water undesirable color [4] and reduce sunlight penetration, with some dyes also being toxic/carcinogenic [5].

A considerable amount of research on wastewater treatment has focused on the elimination of reactive dyes, essentially for three reasons: firstly, reactive dyes represent 20–30% of the total dye market [6]; secondly, large fractions of reactive dyes (10–50%) are wasted during the dyeing process (up to 0.6–0.8 g dye/dm³ can be detected in dyestuff effluent) [7]; thirdly, conventional wastewater treatment methods, which rely on adsorption and aerobic biodegradation, were found to be inefficient for complete elimination of many reactive dyes [1].

Many treatment methods have been adopted to remove dyes from wastewater, which can be divided into physical, chemical,

* Corresponding author.

E-mail address: g.walker@qub.ac.uk (G.M. Walker).

and biological methods [8]. Although chemical and biological methods are effective for removing dyes, they require specialized equipment and are usually quite energy intensive; in addition, large amounts of by-products are often generated [1]. Generally, physical methods which include adsorption, ion exchange, and membrane filtration are effective for removing reactive dyes without producing unwanted by-products [8]. Adsorption of cationic and anionic dyes on activated carbon and by a number of natural adsorbents has been investigated by a number of researchers [9–11].

In this study, the removal of three problematic reactive dyes from water has been investigated using a highly porous, high surface area activated carbon. The physical and chemical characteristics of the activated carbon, including: total pore volume, mesopore volume, micropore volume, surface area, average pore diameter, point of zero charge (pH_{pzc}), and surface functional groups were determined using standard analytical procedures. The acidity constant (K_{a}) of each of the reactive dyes was determined using potentiometric titration. Adsorption isotherms for the reactive dyes were undertaken at $25.0\text{ }^{\circ}\text{C}$ to study the effects of solution pH, ionic strength, and temperature. Based on the modeling of the experimental data a mechanism of interaction between anionic reactive dyes and activated carbon is proposed.

2. Experimental

2.1. Adsorbent and adsorbates

Activated carbon was purchased from the Calgon Company (Pittsburgh, Pennsylvania, USA). The bulk density and the porosity of the adsorbent were 0.64 g/cm^3 and 0.4 , respectively (obtained from the manufacturer), with the elemental analysis of the adsorbent quoted at: C = 86.5%, O = 6.5%, and H = 1.2% (w/w). Three reactive dyes which have a wide industrial application were selected, namely; C.I. Reactive Blue 2; C.I. Reactive Red 4; and C.I. Reactive Yellow 2 (Aldrich Chemicals). The chemical structures of the dyes are illustrated in Fig. 1.

2.2. Chemical and physical characteristics of activated carbon

K_{a} values of reactive dyes were determined according to a standard procedure [12]. The Boehm method which is widely used for determination of acidic and basic surface groups of activated carbons was also used to characterize the activated carbon [13]. Furthermore, the pH_{pzc} was determined using the pH drift method [10].

The textural characteristics of activated carbon including surface area, pore volume, pore size distribution were determined using standard N_2 -adsorption techniques (Nova 4200e, Surface Area and Pore Size Analyzer) [14].

2.3. Reactive dye adsorption isotherms

Equilibrium adsorption isotherms for reactive dyes were undertaken at $25 \pm 1\text{ }^{\circ}\text{C}$. A mass of $0.250 \pm 0.001\text{ g}$ of activated

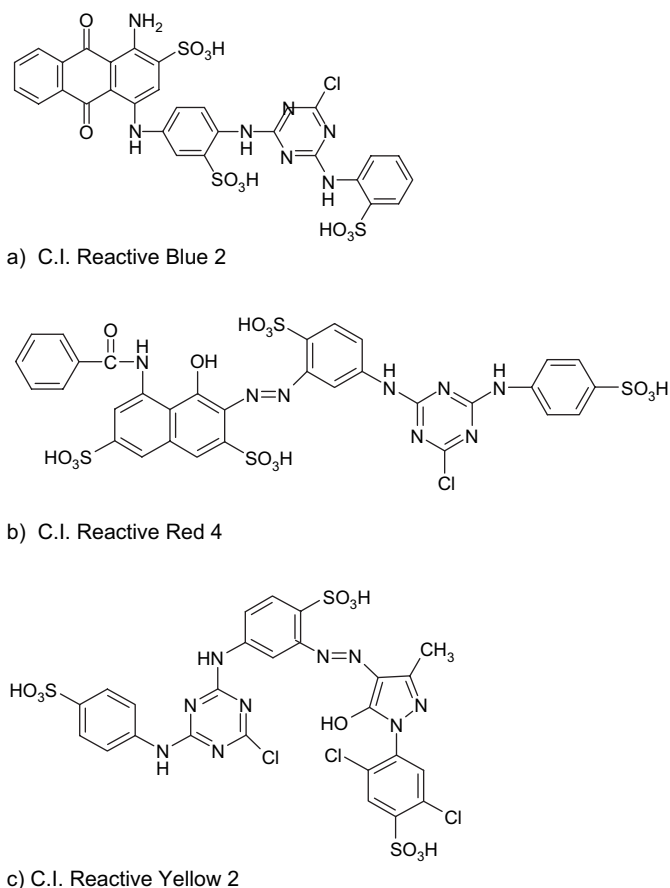


Fig. 1. Chemical structures of reactive dyes.

carbon (particle diameter $300\text{--}500\text{ }\mu\text{m}$) was added to 250 cm^3 bottles containing 100.0 cm^3 of reactive dye of varying concentration: $1.0 \times 10^{-5}\text{--}1.2 \times 10^{-3}\text{ mol/dm}^3$. The bottles were sealed and placed in a thermostated shaker (GFL 1083, Germany) for one week until equilibrium was achieved. The adsorption behavior of the reactive dyes on the activated carbon was studied at four temperatures (298, 308, 318, and 328 K). The adsorption equilibrium isotherm experiments were repeated in duplicate and the average values are reported.

2.4. Effect of solution pH and ionic strength on reactive dye adsorption

The effect of solution pH and ionic strength on dye adsorption was investigated according to the following procedure. A mass of 0.250 g of dried activated carbon ($300\text{--}500\text{ }\mu\text{m}$ particle diameter) was added to a number of 250 cm^3 glass bottles containing 100.0 cm^3 of $6.0 \times 10^{-4}\text{ mol/dm}^3$ dye solution. The pH of the dye solutions was adjusted over the range pH 2–pH 10 using 0.5 M HNO_3 or 0.5 M NaOH solutions (prior to the addition of the adsorbent). The bottles were sealed and placed in the shaker at $25 \pm 1\text{ }^{\circ}\text{C}$ for seven days. The effect of ionic strength on the adsorption of the dyes was investigated according to the following procedure. A mass of 0.250 g of activated carbon ($300\text{--}500\text{ }\mu\text{m}$ particle diameter) was added to 1000 cm^3 solutions of $6.0 \times 10^{-4}\text{ mol/dm}^3$ of dye with varying

concentrations of NaCl (0.05–0.5 mol/dm³). After seven days, the solution phase dye concentration was determined, as described in Section 2.3.

3. Results and discussion

3.1. Dye characterization

Table 1 summarizes the characteristics of the reactive dyes. The acidity constants (K_a) for these particular dyes have not been previously reported. The values of pK_a of the reactive dyes were determined using a standard potentiometric titration method [12]. Due to their acid–base properties, dyes can be titrated using suitable acid or base solution. The pK_a values of reactive dyes were calculated by plotting the equilibrium pH against buffer intensity of dyes (M pH^{−1}) [12]. Fig. 2 illustrates the variations in buffer intensity of C.I. Reactive Blue 2 against pH. pK_a values were obtained from the maximum buffer intensity when the concentration of ionized and neutral dye species was equal [12]. As shown in Fig. 2, the pK_a value of C.I. Reactive Blue 2 was 5.5. Similar curves (not presented) were obtained for the C.I. Reactive Yellow 2 and C.I. Reactive Red 4 dyes. It was found that the reported pK_a values of reactive dyes were similar to those reported for other anionic dyes [15]. Table 1 summarizes the number of polar and ionizable functional groups that were present in dye molecules and contain much the same density of polar functional groups (15–18 groups/molecule) and ionizable groups (3–4 groups/molecule).

3.2. Adsorbent characterization

3.2.1. Chemical characteristics

The surface functional groups and pH_{pzc} are important characteristics for any activated carbon as they indicate: the acidity/basicity of the adsorbent, type of activated carbon (either H- or L-type), and the net surface charge of the carbon in solution. Table 2 summarizes the result of the Boehm titration method, the data indicate that the activated carbon has both basic and acidic properties. The acid functional groups are carboxylic, lactonic, and phenolic [16]. The basic functional groups include oxygen-containing species such as ketonic, pyronic, chromenic, and π -electron system of carbon basal planes [16,17]. The activated carbon has more basic properties and has a relatively low density of surface functional groups (0.54 group/nm²). A value of 14.9 group/nm² has been reported for an activated carbon [16]. The density of surface functional

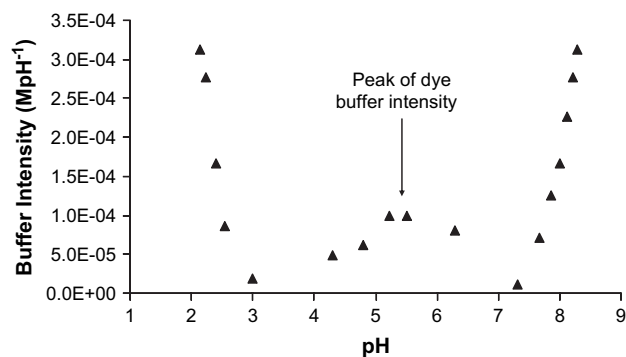


Fig. 2. Buffer intensity curve for C.I. Reactive Blue 2.

groups depends on the activated carbon preparation conditions and on the nature of the precursor [18]. Many chemical treatment procedures have been employed to increase the density of surface functional groups of activated carbon, highlighting the importance of functional group interaction with polar solutes from solution [19]. The combined influence of all the functional groups of activated carbon determines pH_{pzc} , i.e., the pH at which the net surface charge on carbon was zero. At $pH < pH_{pzc}$, the carbon surface has a net positive charge, while at $pH > pH_{pzc}$ the surface has a net negative charge [20]. Fig. 3 shows the “pH drift” data, from which the pH_{pzc} of the adsorbent can be determined (pH 9.0). The pH_{pzc} is the point where the curve pH_{final} vs $pH_{initial}$ intersects the line $pH_{initial} = pH_{final}$ [10].

3.2.2. Physical characteristics

The textural characteristics of activated carbon obtained from N₂-adsorption analysis are summarized in Table 3, indicating that the adsorbent has a large specific surface area (820 m²/g) typical for commercial activated carbons [24]. Comparing the magnitude of the total surface area with the surface area of micropores indicates the high microporosity of the adsorbent. The area of the micropores contributes to 86% of the total surface area. The high microporosity of the adsorbent was evident when comparing the micropore volume with the total pore volume. The micropore volume contributes to about 82% of the total pore volume. The percentage microporosity can be further increased using a number of chemical procedures; the percentage microporosity can increase to 99% for an activated carbon after treatment by NaOH solution [25]. Normally, pores of adsorbents can be divided into micropores (pore diameter < 2 nm), mesopores (pore diameter range 2–50 nm), and

Table 1
Characteristics of reactive dyes

C.I. generic name	λ_{max} (nm)	Solubility at 25 °C (g/dm ³) ^a	pK_a	C (wt%)	Number of ionizable groups	Number of polar functional groups located on dyes that can interact with activated carbon				
						–S–O	–C–O	–Cl	–NH	–NH ₂
Reactive Blue 2	604.0	60.0	5.5	45.0	3	9	2	1	3	1
Reactive Red 4	517.0	120.0	4.4	38.6	4	12	2	1	3	–
Reactive Yellow 2	404.0	70.0	5.3	34.5	3	9	1	3	2	–

^a Manufacturer data.

Table 2
Acidity/basicity and pH_{pzc} of activated carbon^a

Total basic groups (mmol/g)	Total acidic groups (mmol/g)	Carboxylic groups (mmol/g)	Lactonic groups (mmol/g)	Phenolic groups (mmol/g)	Total functional groups (mmol/g)	Density of groups on the surface ^b (group/nm ²)	pH _{pzc}
0.43	0.30	0.06	0.08	0.16	0.73	0.54	9.0

^a All the reported results are average of three trials.

^b Specific surface area = 820 m²/g.

macropores (pore diameter > 50 nm) [24]. As shown in Table 3, the average pore diameter for this activated carbon was 1.8 nm as obtained from Barrett–Joyner–Hanlenda (BJH) method [21], which also indicates that the adsorbent was highly microporous.

3.3. Equilibrium isotherms for reactive dye adsorption on activated carbon

Adsorption isotherm data of the reactive dyes are illustrated in Fig. 4. The shape of the isotherms indicates L2-behavior according to Giles and Smith classification [26]. In L2-type isotherms, adsorption of solute on the adsorbent proceeds until a monolayer is established, with the formation of more than one layer not being possible [26]. The shape of isotherm presented in Fig. 4 is indicative of high affinity between the sorbent surface and the reactive dye molecules. The adsorbent effectively removes the three dyes at low initial concentrations; at higher concentrations the isotherms reach a maximum capacity as indicated by the plateau of the data. Most reported adsorption isotherms of reactive dyes were of L2-type isotherm [4,5,10,27]. L2-type isotherms are usually associated with ionic solute adsorption (e.g., metal cations and ionic dyes) with weak competition with the solvent molecules [26]. Accordingly, the anionic reactive dye molecules favorably adsorb on the carbon surface with low competition from water molecules, with this adsorption process continuing until the surface concentration reaches a maximum value. In addition, the formation multi-layers of adsorbate was not possible due to the electrostatic repulsion between adsorbed molecules and those in solution [26].

3.3.1. Langmuir and Freundlich equilibrium isotherm models

The correlation of the experimental adsorption data with a number of adsorption models was undertaken to gain an

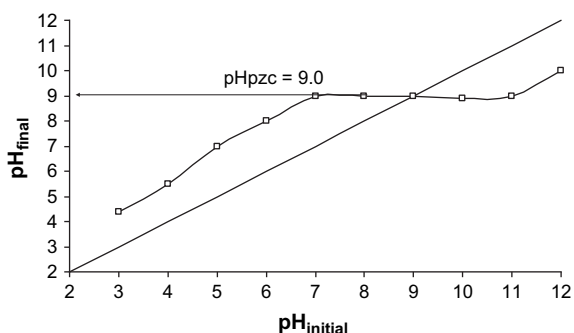


Fig. 3. Determination of pH_{pzc} of activated carbon by the pH drift method [10].

understanding of the adsorption behavior and the heterogeneity of the adsorbent surface. The Langmuir equation can be represented as follows [28]:

$$q_e = \frac{Q_{\max} K_L C_e}{1 + K_L C_e} \quad (1)$$

where: C_e (mmol/dm³) is the equilibrium concentration of dye in solution; q_e (mmol/g) is the surface concentration of dye at equilibrium; Q_{\max} (mmol/g) is the amount of dye adsorbed at complete monolayer coverage; K_L (dm³/mmol) is a constant that relates to the heat of adsorption [24].

The Freundlich model can take the following form [28]:

$$q_e = K_F C_e^n \quad (2)$$

where: K_F [mmol/g (mmol/dm³)⁻ⁿ] represents the adsorption capacity when dye equilibrium concentration (C_e) equals 1; n represents the degree of dependence of adsorption on equilibrium concentration. The model parameters (as obtained from linear-regression analysis) and correlation coefficients (r^2) are presented in Table 4.

3.3.1.1. Langmuir model. The correlation of the dye adsorption data with the Langmuir isotherm model was high, with r^2 values of 0.9912, 0.9712 and 0.9735 for C.I. Reactive Blue 2, C.I. Reactive Yellow 2 and C.I. Reactive Red 4 dyes, respectively. As shown in Table 4, the maximum adsorption values for the dyes were 0.27 and 0.24 and 0.11 mmol/g for C.I. Reactive Blue 2, C.I. Reactive Yellow 2, and C.I. Reactive Red 4, respectively. K_L represents the equilibrium adsorption constant, therefore higher values of K_L were indicative of a favorable adsorption process. By comparing the values of K_L , it can be

Table 3
Textural characteristics of activated carbon

S_{BET}^a (m ² /g)	S_{external}^b (m ² /g)	S_{mic}^c (m ² /g)	Total pore volume ^d (cm ³ /g)	Micropore volume ^e (cm ³ /g)	Mesopore volume ^f (cm ³ /g)	Average pore diameter ^g (nm)
820	110	710	0.56	0.46	0.10	1.8

^a Specific surface area (multipoint BET method [21]).

^b External surface area (t -plot method [21]).

^c Micropore surface area (t -plot method [21]).

^d Calculated from the amount of N₂ adsorbed at $P/P_0 = 0.95$ [22].

^e Obtained from Dubinin–Radushkevich method [14].

^f Calculated from the amount of N₂ adsorbed between relative pressure P/P_0 : 0.40–0.95 assuming that the molar volume of liquid nitrogen is 35 cm³/mol [23].

^g Obtained from Barrett–Joyner–Hanlenda (BJH) method [21].

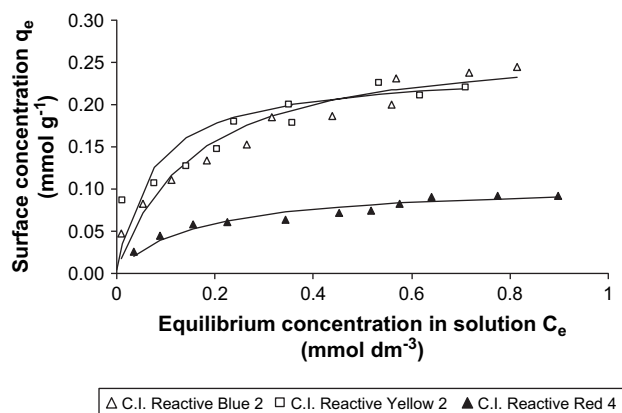


Fig. 4. Adsorption isotherms of reactive dyes. Mass of carbon: 0.25 g; volume of solution: 100.0 cm³; pH: 7; dye concentration range: 1.0×10^{-4} – 1.2×10^{-3} mol/dm³; temperature: 25.0 °C. Points: experimental data; lines: Langmuir model.

concluded that adsorption of C.I. Reactive Blue 2 and C.I. Reactive Yellow 3 dyes ($K_L = 6.6$ and 5.4) was more favorable than that of C.I. Reactive Red 4 ($K_L = 3.2$). The fraction of the carbon surface that is occupied by dye molecules (θ) can be calculated from the amount of dye adsorbed and the surface area occupied by one dye molecule (σ) using the following equation [22,29]:

$$\theta = \frac{Q_{\max} N \sigma \times 10^{-20}}{S_{\text{BET}}} \quad (3)$$

where: θ represents the fraction of the surface that is occupied by dye molecules at saturation; Q_{\max} (mol/g) is the amount of dye adsorbed at saturation, as obtained from the Langmuir model; σ (Å²/molecule) is the surface area occupied by one molecule; N is the Avogadro's number (6.022×10^{23}); S_{BET} is the specific surface area of the adsorbent (820 m²/g). McClellan and Harnsberger have proposed an empirical relationship that may be used for the estimation of σ of organic molecules adsorbed on activated carbon [30]:

$$\sigma \left(\text{\AA}^2/\text{molecule} \right) = 1.091 \times 10^{16} \left(\frac{\text{MW}}{\rho N} \right)^{2/3} \quad (4)$$

where: MW is the molar mass of the adsorbed molecule (g/mol); ρ is the adsorbate density (g/cm³). The corresponding values of σ and θ for reactive dyes are given in Table 5. The values of θ were 0.45, 0.42, and 0.22 for C.I. Reactive Blue 2, C.I.

Reactive Yellow 2 and C.I. Reactive Red 4 dyes, respectively. The values of θ indicate that the formation of a complete molecular layer ($\theta = 1$) was not achieved for the three dyes and a large fraction of the adsorbent surface remains unoccupied, particularly in the case of C.I. Reactive Red 4. The incomplete formation of a monolayer may be attributed to large molecular diameter of the dye molecules which cannot fully access the sorbent micropores that account for about 87% of the total surface area of the adsorbent (see Table 3).

3.3.1.2. Freundlich model. The model parameters and r^2 values are presented in Table 4, which indicate that this model showed lower correlation with the experimental adsorption data compared to the Langmuir model. The extent of adsorption for C.I. Reactive Blue 2 was approximately three times that of C.I. Reactive Red 4, as inferred from the values of K_F , 0.30 and 0.10, respectively. The high adsorption capacity of C.I. Reactive Blue 2 compared to C.I. Reactive Red 4 can also be illustrated from the values of Q_{\max} using the Langmuir model. The n values for all adsorption systems studied were less than unity, which reflects the favorable adsorption of the reactive dyes over the entire concentration range used in this study (1.0×10^{-4} – 1.2×10^{-3} mol/dm³) [31]. Furthermore, the surface of activated carbon is known to be highly heterogeneous and the energies of active sites are highly variable, which would also tend to make the values of n less than unity [22,32].

3.4. Effect of solution pH and ionic strength on dye adsorption and identification of the adsorption mechanism

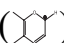
The effect of solution pH on dye removal from solution was studied under identical conditions for the three dyes chosen for this study. The data are presented in Fig. 5, which indicate that the adsorption behavior of each of the reactive dyes was similar, from pH 2 to pH 10, (e.g., the removal of C.I. Reactive Blue 2 decreased from 70% to 56%, when the pH was increased from 2 to 4, with the percentage removal then remaining almost constant up to pH 8). A large decrease in adsorption capacity for this dye was observed under basic conditions (i.e., a decrease to 40% removal at pH 10). Similar adsorption behavior with variation in solution pH has been reported in the literature [2,33]. If electrostatic interaction was the only mechanism for the dye adsorption, then the removal capacity should

Table 4
Model parameters obtained from fitting the experimental equilibrium data with isotherm models

C.I. Reactive Blue 2				
Langmuir isotherm	C_e (mmol/dm ³): 0.1–0.8	$K_L = 6.6$	$Q_m = 0.27$	$r^2 = 0.9912$
Freundlich isotherm	C_e (mmol/dm ³): 0.1–0.8	$K_F = 0.30$	$n = 0.38$	$r^2 = 0.9635$
C.I. Reactive Yellow 2				
Langmuir isotherm	C_e (mmol/dm ³): 0.1–0.8	$K_L = 5.4$	$Q_m = 0.24$	$r^2 = 0.9712$
Freundlich isotherm	C_e (mmol/dm ³): 0.1–0.8	$K_F = 0.23$	$n = 0.25$	$r^2 = 0.9622$
C.I. Reactive Red 4				
Langmuir isotherm	C_e (mmol/dm ³): 0.2–0.9	$K_L = 3.2$	$Q_m = 0.11$	$r^2 = 0.9735$
Freundlich isotherm	C_e (mmol/dm ³): 0.2–0.9	$K_F = 0.10$	$n = 0.37$	$r^2 = 0.9591$

Table 5
Values of σ and θ for adsorbed reactive dyes

Dye	Density (g/cm ³)	MW (g/mol)	Q_{\max} (mmol/g) (at 25 °C)	σ (Å ² /molecule)	θ
C.I. Reactive Blue 2	0.423	773.5	0.27	228.8	0.45
C.I. Reactive Yellow 2	0.445	872.5	0.24	239.7	0.42
C.I. Reactive Red 4	0.415	994.5	0.11	273.9	0.22

be at a maximum within the range pH 6–8. In this pH range the surface of activated carbon is positively charged ($\text{pH}_{\text{pzc}} = 9.0$) and dyes are negatively charged (pK_{a} of dyes 4.4–5.5). The protonated groups of activated carbon are mainly carboxylic group ($-\text{CO}-\text{OH}_2^+$), phenolic ($-\text{OH}_2^+$) and chromenic groups () [16,17,20]. The deprotonated groups of the dye were probably the sulphonate groups ($-\text{SO}_3^-$). At solution $\text{pH} \leq 4$, the removal capacity was expected to decrease, as the adsorbent was positively charged and dye molecules were either neutral or partially positively charged. At this acidic pH, the sulphonate groups of the dyes were almost protonated ($-\text{SO}_3\text{H}$, i.e., neutral). Furthermore, the protonation of nitrogen atoms especially those not involved in aromatic systems is also probable. The large reduction in dye adsorption at highly basic conditions can be attributed to electrostatic repulsion between the negatively charged activated carbon and the deprotonated dye molecules. The constant adsorption capacity of activated carbon for dyes over the pH range 4–8 was an indication that the electrostatic mechanism was not the only mechanism for dye adsorption in this system. Activated carbon can also interact with dye molecules via hydrogen bonding and hydrophobic–hydrophobic mechanisms [23,34].

As shown in Fig. 6, adsorption of reactive dyes on activated carbon increased upon addition of small quantities of salt, however, this increase plateaued at a salt concentration of 0.1 mol/dm³. The effect of ionic strength on dye adsorption was studied at pH 7.0, where dyes and activated carbon were oppositely charged ($\text{pH}_{\text{pzc}} = 9.0$ of activated carbon and pK_{a} 4.4–5.5 of dyes). Theoretically, when the electrostatic forces between

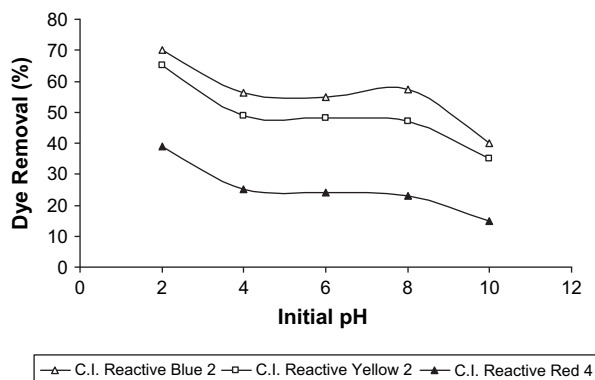


Fig. 5. Effect of solution pH on extent of dye adsorption. Experimental conditions: initial dye concentration 0.6 mmol/dm³; carbon mass 0.25 g; volume of solution 100 cm³; temperature 25.0 °C.

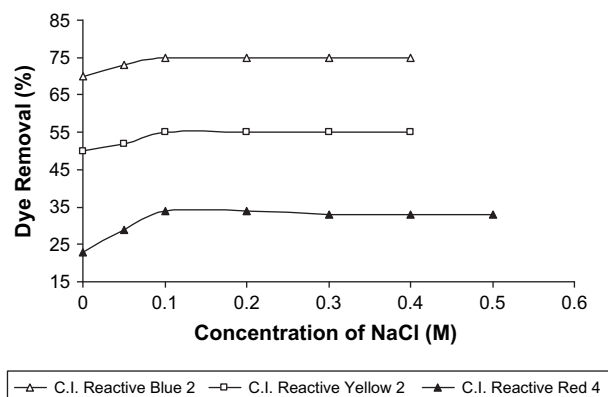


Fig. 6. Effect of solution ionic strength on the extent of dye adsorption. Experimental conditions: initial dye concentration 0.6 mmol/dm³; mass of carbon 0.250 g; volume of solution 100 cm³; temperature 25.0 °C; pH 7.0.

the adsorbent surface and adsorbate ions were attractive, as in this system, an increase in ionic strength will decrease the adsorption capacity. Conversely, when the electrostatic attraction is repulsive, an increase in ionic strength will increase adsorption [23,35,36]. The experimental data from this study did not follow this convention, as the adsorption of negatively charged dye molecules on positively charged activated carbon increased with NaCl addition. The significant increase in dye removal after NaCl addition can be attributed to an increase in dimerization of reactive dyes in solution. The effect of salt and temperature on the dimerization of reactive dyes has been extensively investigated by Alberghina and co-workers [35]. A number of intermolecular forces have been suggested to explain this aggregation, these forces include: van der Waals forces; ion–dipole forces; and dipole–dipole forces, which occur between dye molecules in the solution. It has been reported that these forces increased upon the addition of salt to the dye solution [35]. Accordingly, the higher adsorption capacity of reactive dyes under these conditions can be attributed to the aggregation of dye molecules induced by the action of salt ions, i.e., salt ions force dye molecules to aggregate, increasing the extent of sorption on the carbon surface. In a similar study, Germán-Heins and Flury have reported an increase in Brilliant Blue (a reactive dye) adsorption after adding salt to the solution [36]. It is important to note that the absorption characteristics and λ_{\max} of dyes were insensitive to changes in pH and ionic strength of solution.

3.5. Effect of temperature on dye adsorption and thermodynamics

The adsorption of C.I. Reactive Blue 2 and C.I. Reactive Yellow 2 on activated carbon was studied at temperatures of 298, 308, 318 and 328 K, with these adsorption isotherms being shown in Figs. 7 and 8. The free energy of adsorption (ΔG_{ads}) was calculated from the following equation [37]:

$$\Delta G = -RT \ln K_{\text{L1}} \quad (5)$$

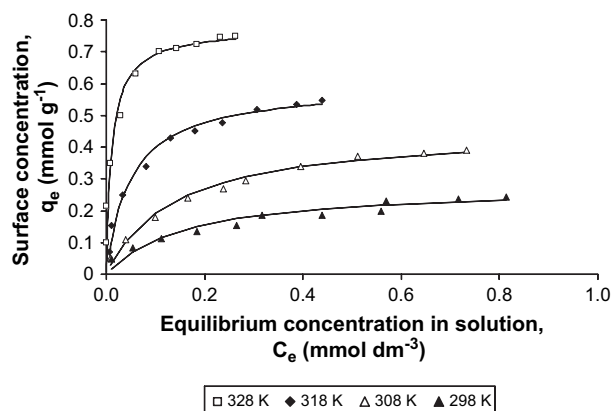


Fig. 7. Adsorption isotherms of C.I. Reactive Blue 2 on activated carbon at different temperatures. Carbon mass 0.25 g; volume of solution 100.0 cm³; pH 7; dye concentration range 1.0×10^{-5} – 2.0×10^{-3} mol/dm³. Points: experimental data, lines: Langmuir model.

where: K_{L1} is the Langmuir constant at T_1 ; R is the gas constant (8.314 J/mol K). The apparent enthalpy of adsorption, (ΔH_{ads}), and entropy of adsorption, (ΔS_{ads}), were calculated from adsorption data at different temperatures using the Van't Hoff equation [33]:

$$\ln(K_L) = \frac{\Delta S}{R} - \frac{\Delta H}{RT} \quad (6)$$

where: K_L is the Langmuir constant and T is the solution temperature (K). The magnitude of ΔH_{ads} and ΔS_{ads} was calculated from the slope and y-intercept from the plot of $\ln K_L$ vs $1/T$, with these thermodynamic parameters being given in Table 6.

As shown in Figs. 7 and 8, the adsorption capacity of both dyes increased at higher temperatures, which indicates that adsorption of dyes in this system was an endothermic process. For both dyes, the surface coverage increased at higher

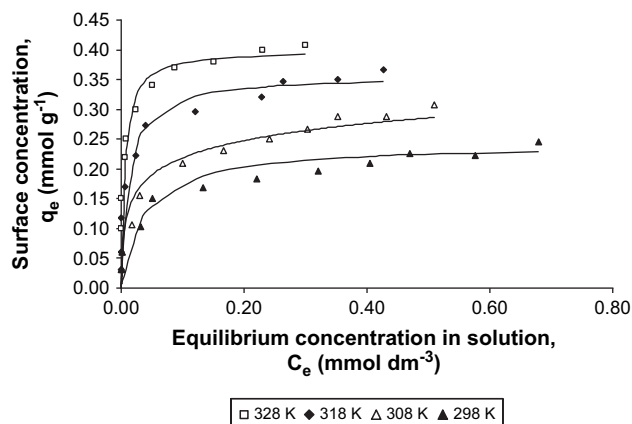


Fig. 8. Adsorption isotherms of C.I. Reactive Yellow 2 on activated carbon at different temperatures. Carbon mass 0.25 g; volume of solution 100.0 cm³; pH 7; dye concentration range 1.0×10^{-5} – 1.2×10^{-3} mol/dm³. Points: experimental data, lines: Langmuir model.

temperatures (see Table 6), this may be attributed to increased penetration of reactive dyes inside micropores at higher temperatures or the creation of new active sites. The formation of more than one molecular layer on the surface of activated carbon appears to be achieved in the case of C.I. Reactive Blue 2 dye adsorption at 328 K where the value of θ was 1.30. ΔH_{ads} values as calculated from Eq. (6) were +37.2 and +34.1 kJ/mol for C.I. Reactive Blue 2 and C.I. Reactive Yellow 2, respectively. Physical adsorption and chemisorption can be classified, to a certain extent, by the magnitude of the enthalpy change. It is accepted that bonding strengths of <84 kJ/mol are typically those of physical adsorption type bonds. Chemisorption bond strengths can range from 84 to 420 kJ/mol [38]. Based on this, the adsorption of reactive dyes on activated carbon appears to be a physical adsorption process. However, the enthalpy ranges quoted above were derived from gaseous adsorption studies and may not strictly apply for adsorption from solution. Some researchers have suggested that sorption from aqueous solution onto activated carbon is by a different adsorption mechanism, which may not be described as either physical adsorption or chemisorption [18]. The enthalpy of adsorption of organic molecules from aqueous solution on activated carbon is usually within the range 8–65 kJ/mol [18].

Moreover it was expected that adsorption processes (either from gas or liquid phase) are exothermic due to the heat released after bond formation between solute and adsorbent [18,24,38]. The endothermic adsorption of reactive dyes on activated carbon appears to be uncommon behavior, however, several authors have reported endothermic adsorption of reactive dyes on different types of adsorbents [2,27,33,39]. The adsorption of reactive dyes was spontaneous at the temperatures under investigation as indicated from the negative values of free energy (ΔG_{ads}).

4. Conclusions

Activated carbon with a large surface area (820 m²/g) and a modest surface charge density (0.54 group/nm²) was shown to be effective in removing anionic reactive dyes from solution. At pH 7.0 and 298 K, the maximum adsorption values as described using the Langmuir equilibrium isotherm model were 0.27, 0.24, and 0.11 mmol/g for C.I. Reactive Blue 2, C.I. Reactive Yellow 2 and C.I. Reactive Red 4 dyes, respectively. The formation of a complete monolayer was not achieved and the fraction of surface coverage was calculated as 0.45, 0.42, and 0.22 for C.I. Reactive Blue 2, C.I. Reactive Yellow 2 and C.I. Reactive Red 4 dyes, respectively. The adsorption capacity of the dyes on activated carbon increased in acidic solutions, but decreased in basic solutions. The adsorption capacity of the dyes increased when increasing the ionic strength of solution, this was attributed to dye aggregation in solution. Adsorption of reactive dyes was found to be spontaneous at the temperatures under investigation (298–328 K) as indicated from the negative values of free energy (ΔG_{ads}).

Table 6

Thermodynamic parameters for reactive dye adsorption on activated carbon under different temperatures

C.I. Reactive Blue 2						C.I. Reactive Yellow 2				
<i>T</i> (K)	<i>K_L</i>	<i>Q_{max}</i> (mmol/g)	ΔG_{ads} (kJ/mol)	ΔH_{ads} (kJ/mol) ^a	ΔS_{ads} (J/mol K)	<i>Q_{max}</i> (mmol/g)	<i>K_L</i>	ΔG_{ads} (kJ/mol)	ΔH_{ads} (kJ/mol) ^b	ΔS_{ads} (J/mol K)
298	6.6	0.27	−4.7	37.2	140.5	0.24	5.5	−4.2	34.1	128.9
308	12.2	0.39	−6.4			0.31	8.7	−5.5		
318	18.3	0.52	−7.7			0.37	13.8	−6.9		
328	26.4	0.77	−8.9			0.41	19.0	−8.0		

^a Results of plotting $\ln K_L$ vs $1/T$ (Eq. (6)): slope = −4475, intercept = 16.9, $r^2 = 0.9922$.^b Results of plotting $\ln K_L$ vs $1/T$ (Eq. (6)): slope = −4100, intercept = 15.5, $r^2 = 0.9967$.

References

- [1] Robinson T, McMullan G, Marchant R, Nigam P. Remediation of dyes in textile effluent: a critical review on current treatment technologies with a proposed alternative. *Bioresource Technology* 2001;77:247–55.
- [2] Netpradit S, Thiravetyan P, Towprayoon S. Adsorption of three azo reactive dyes by metal hydroxide sludge: effect of temperature, pH, and electrolytes. *Journal of Colloid and Interface Science* 2004;270:255–61.
- [3] Mottaleb M, Littlejohn D. Application of an HPLC–FTIR modified thermospray interface for analysis of dye samples. *Analytical Sciences* 2001;17:429–34.
- [4] Al-Degs YS, El-Barghouthi MI, Khraisheh MA, Ahmad MN, Allen SJ. Effect of surface area, micropores, secondary micropores and mesopores volumes of activated carbons on reactive dyes adsorption from solution. *Separation Science and Technology* 2004;39:97–111.
- [5] Wang S, Boyjoo Y, Choueib A, Zhu H. Removal of dyes from solution using fly ash and red mud. *Water Research* 2005;39:129–38.
- [6] Órfão J, Silva A, Pereira J, Barata S, Fonseca I, Faria P, et al. Adsorption of a reactive dye on chemically modified activated carbons—influence of pH. *Journal of Colloid and Interface Science* 2006;296:480–9.
- [7] Al-Duri B, Khader K, McKay G. Prediction of binary compound isotherm for adsorption on heterogeneous surfaces. *Journal of Chemical Technology and Biotechnology* 1992;53:345–52.
- [8] Vandevivere P, Bianchi R, Verstraete W. Review: treatment and reuse of wastewater from the textile wet-processing industry: review of emerging technologies. *Journal of Chemical Technology and Biotechnology* 1998;72:289–302.
- [9] Janoš P, Buchtová H, Milena Rýznarová M. Sorption of dyes from aqueous solutions onto fly ash. *Water Research* 2003;37:4938–44.
- [10] Faria P, Órfão J, Pereira M. Adsorption of anionic and cationic dyes on activated carbons with different surface chemistries. *Water Research* 2004;38:2043–52.
- [11] Crini G. Non-conventional low-cost adsorbents for dye removal: a review. *Bioresource Technology* 2006;97:1061–85.
- [12] Wang J, Huang C, Allen H, Cha D, Kim D. Adsorption characteristics of dye onto sludge particulates. *Journal of Colloid and Interface Science* 1998;208:518–28.
- [13] Boehm H. Some aspects of the surface chemistry of carbon blacks and other carbons. *Carbon* 1994;32:759–69.
- [14] Güzel F, Tez Z. The characterization of the micropore structure of some activated carbon of plant origin by N_2 and CO_2 adsorption. *Separation Science and Technology* 1993;28:1609–27.
- [15] Lorenc-Grabowska E, Gryglewicz G. Adsorption characteristics of Congo Red on coal-based mesoporous activated carbon. *Dyes and Pigments* 2007;74:34–40.
- [16] Chun Y, Sheng G, Chiou C, Xing B. Compositions and sorptive properties of crop residue-derived chars. *Environmental Science and Technology* 2004;38:4649–55.
- [17] Leon Y, Leon C, Solar J, Calemma V, Radovic L. Evidence for the protonation of basal plane sites on carbon. *Carbon* 1992;30:797–811.
- [18] Mattson J, Mark H. Activated carbon: surface chemistry and adsorption from solution. New York: Marcel Dekker, Inc.; 1971.
- [19] Mazet M, Farkhani B, Baudu M. Influence of heat or chemical treatment of activated carbon onto the adsorption of organic compounds. *Water Research* 1994;28:1609–17.
- [20] Al-Degs Y, Khraisheh M, Allen S, Ahmad M. Effect of carbon surface chemistry on the removal of reactive dyes from textile effluents. *Water Research* 2000;34:927–35.
- [21] Gregg S, Sing K. Adsorption, surface area and porosity. 2nd ed. Academic Press; 1982.
- [22] Haghseresh H, Lu G. Adsorption characteristics of phenolic compounds onto coal-rejected-derived adsorbents. *Energy and Fuels* 1998;12:1100–7.
- [23] Newcombe G, Drikas M. Adsorption of NOM activated carbon: electrostatic and non-electrostatic effects. *Carbon* 1997;35:1239–50.
- [24] Ruthven DM. Principles of adsorption and adsorption processes. A Wiley-Interscience publication, John Wiley and Sons; 1984.
- [25] Lillo-Ródenas M, Fletcher A, Thomas K, Cazorla-Amorós D, Linares-Solano A. Competitive adsorption of a benzene–toluene mixture on activated carbons at low concentration. *Carbon* 2006;44:1455–63.
- [26] Giles C, Smith D. General treatment and classification of the solute sorption isotherms. *Journal of Colloid and Interface Science* 1974;47:755–65.
- [27] Moreira R, Kuhnen N, Peruch M. Adsorption of reactive dyes onto granular activated carbon. *Latin American Applied Research* 1998;28:37–41.
- [28] Chatzopoulos D, Varma A, Irvine R. Activated carbon adsorption and desorption of toluene in the aqueous phase. *AIChE Journal* 1993;39:2027–41.
- [29] Gusler G, Browne T, Cohen Y. Sorption of organics from aqueous solution onto polymeric resins. *Industrial and Engineering Chemistry Research* 1993;32:2727–35.
- [30] McClellan A, Harnsberger H. Cross-sectional areas of molecules adsorbed on solid surfaces. *Journal of Colloid and Interface Science* 1967;23:577–99.
- [31] Frimmel F, Huber L. Influence of humic substances on the aquatic sorption of heavy metals on defined minerals phases. *Environment International* 1996;22:507–17.
- [32] Yang X, Al-Duri B. Kinetic modeling of liquid-phase adsorption of reactive dyes on activated carbon. *Journal of Colloid and Interface Science* 2005;287:25–34.
- [33] Namasivayam C, Kavitha D. Removal of Congo Red from water by adsorption onto activated carbon prepared from coir pith, an agricultural solid waste. *Dyes and Pigments* 2002;54:47–58.
- [34] Newcombe G, Donati C, Drikas M, Hayes R. Adsorption onto activated carbon: electrostatic and non-electrostatic interactions. *Water Supply* 1996;14:129–44.
- [35] Alberghina G, Bianchini R, Fichera M, Fisichella S. Dimerization of Cibacron Blue F3GA and other dyes: influence of salts and temperature. *Dyes and Pigments* 2000;46:129–37.
- [36] Germán-Heins J, Flury M. Sorption of Brilliant Blue FCF in soils as affected by pH and ionic strength. *Geoderma* 2000;97:87–101.
- [37] Gupta V, Suhas V, Mohan D. Equilibrium uptake and sorption dynamics for the removal of a basic dye (basic red) using low-cost adsorbents. *Journal of Colloid and Interface Science* 2003;265:257–64.
- [38] Faust S, Aly O. Adsorption processes for water treatment. Butterworth Publishers; 1987.
- [39] Guo Y, Zhao J, Zhang H, Yang S, Qi J, Wang Z, et al. Use of rice husk-based porous carbon for adsorption of Rhodamine B from aqueous solutions. *Dyes and Pigments* 2005;66:123–8.